

Modeling the GRB jet properties with 3D general relativistic simulations of magnetically arrested accretion flows

Bestin James, Agnieszka Janiuk, Fatemeh Hossein Nouri

Center for Theoretical Physics PAS, Warsaw

CPB Meeting, Brno - June 3, 2022



Gamma Ray Bursts

- Gamma Ray Bursts (GRBs) - most energetic events observed in the universe, releasing a total energy of upto 10^{52} - 10^{54} erg/s
- Two classes of GRBs - based on their duration: short and long - GRBs
 - Short GRBs: a few ms to < 2 s
 - Long GRBs: > 2 s to a few hundred seconds
- Usually, different mechanisms explaining the central engine
 - BH-NS or BNS merger for short-GRBs
 - Collapsar scenario for long-GRBs
- Both scenarios can result in an accretion disk around a central black hole

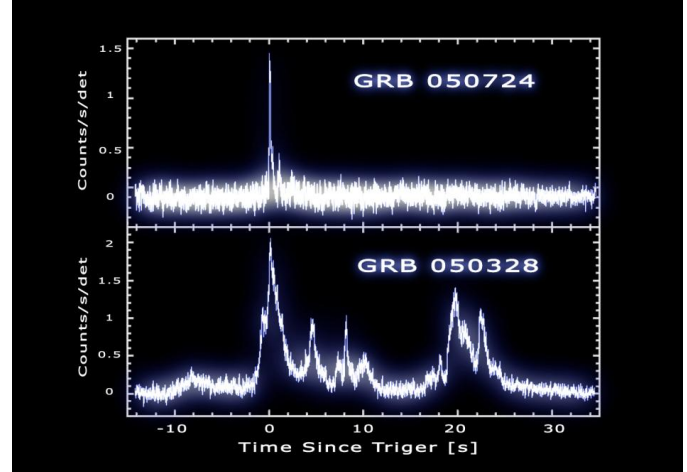
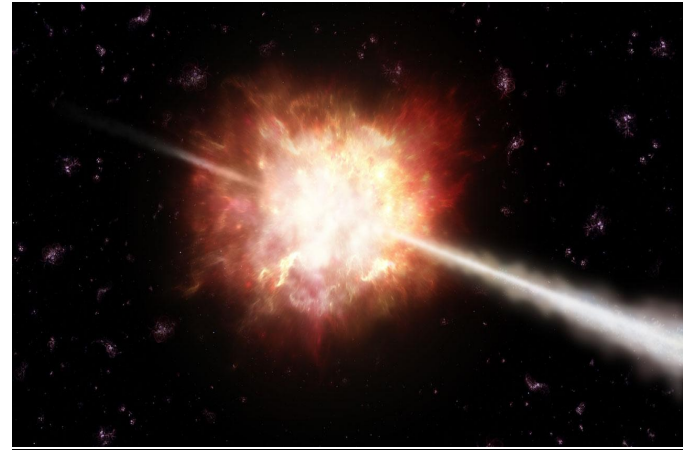
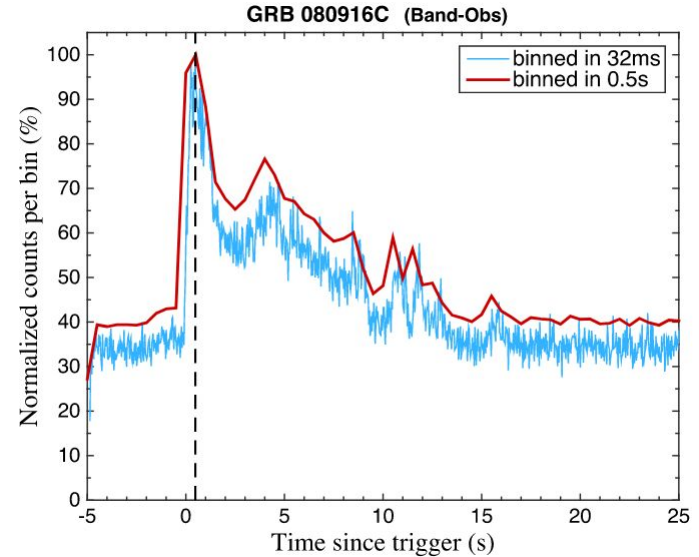


Image Credits: Top: Artist's impression of a GRB - ESO/A. Roquette
Bottom: Light curves of short and long GRBs - NASA

Gamma Ray Bursts

- The origin of high energy emission needs more understanding
- GRBs show very fast variability in time which goes up to sub ms scales. The reasons which are not quite clear
- They show complex jet structures rather than a simple top hat, as was initially assumed
- Jet opening angles span over a wide range of values from a few degrees to over 30 or more



The light curve in the 20–200 keV band of GRB 080916C. The thin (blue) curves are the light curves binned in 0.032 s and the thick (red) curves are those binned in 0.5 s. The y-axis is the normalized counts

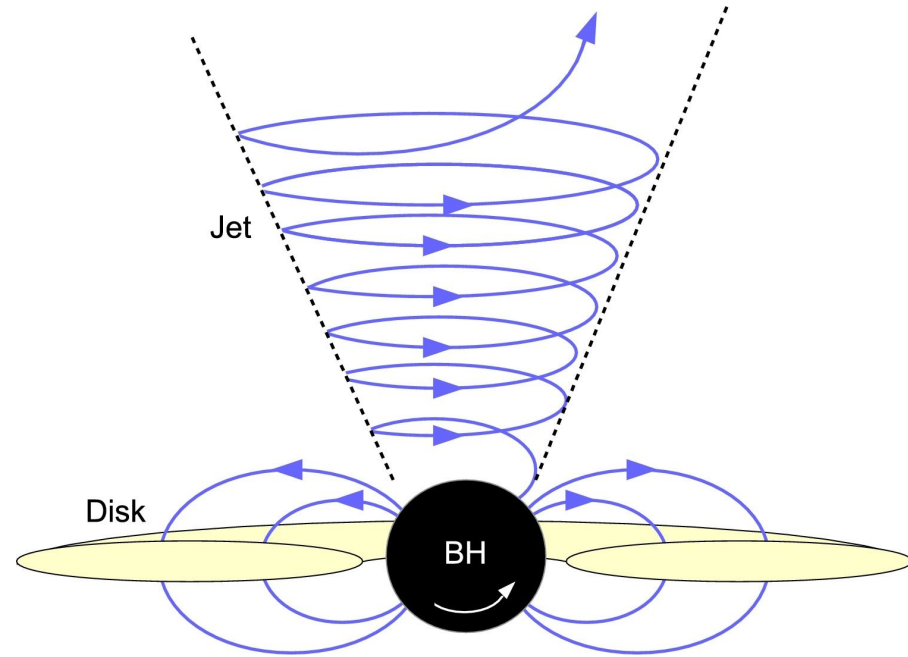
Credit: Yue Liu et al. 2018

Relativistic Jets

- GRBs are observed as relativistic jets pointing towards our line of sight
- Such jets are Poynting-dominated, plausibly powered by the Blandford & Znajek (1977) mechanism which can extract rotational energy from a black hole

$$P_{Bz} \sim \frac{\phi_{BH}^2 \cdot \Omega_{BH}^2}{c}$$

- It is generally assumed that the properties of the central engine affect the jet properties.
- We investigate this with our 3D GRMHD simulations of accretion disks and the associated jet base in a fixed Kerr geometry.



Relativistic jet launching from a black hole-accretion disk system, formed as a result of a BH-NS interaction, through the Blandford-Znajek mechanism. Magnetic field lines (blue) are anchored in the accretion disk (yellow) and penetrate the black hole's ergosphere. Spinning BH twists open field lines, leading to a jet.

Credit: V. Takhistov, 2018

HARM code

We use the HARM code, a conservative, shock capturing scheme, for evolving the equations of GRMHD, originally developed by Gammie et al. (2003).

The code provides a solver for the continuity, energy-momentum conservation and induction equations in GR:

$$\nabla_{\mu}(\rho u^{\mu}) = 0; \quad \nabla_{\mu} T^{\mu\nu} = 0; \quad \nabla_{\mu}(u^{\nu} b^{\mu} - u^{\mu} b^{\nu}) = 0$$

The stress-energy tensor, in general, contains the gas and electromagnetic parts:

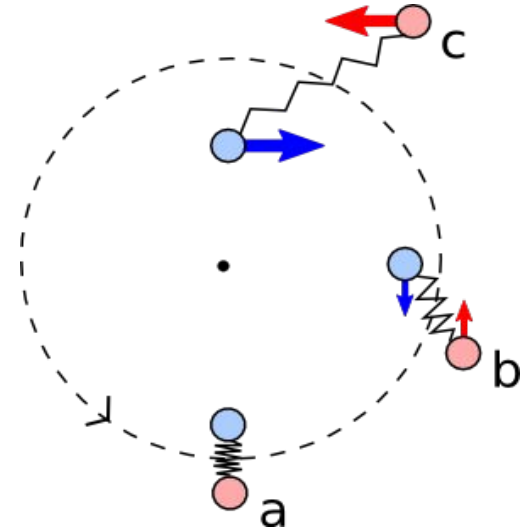
$$\begin{aligned} T^{\mu\nu} &= T_{\text{gas}}^{\mu\nu} + T_{EM}^{\mu\nu} \\ T_{\text{gas}}^{\mu\nu} &= \rho h u^{\mu} u^{\nu} + p g^{\mu\nu} = (\rho + u + p) u^{\mu} u^{\nu} + p g^{\mu\nu} \\ T_{EM}^{\mu\nu} &= b^2 u^{\mu} u^{\nu} + \frac{1}{2} b^2 g^{\mu\nu} - b^{\mu} b^{\nu}; \quad b^{\mu} = u_{\nu}^* F^{\mu\nu} \end{aligned}$$

where u is internal energy, u^{μ} is four-velocity of gas, and $b^{\mu} = \frac{1}{2} \varepsilon^{\mu\nu\rho\sigma} u_{\nu} F_{\rho\sigma}$.

In force-free approximation, $E_{\nu} = u_{\mu} F^{\mu\nu} = 0$. The code works in a GR framework with $G=c=M=1$.

Plasma Instabilities Involved

- **Magnetorotational Instability (MRI):**
 - Originally described by Velikov (1959) and Chandrasekhar (1960).
 - Importance to accretion disks was recognized by Balbus & Hawley (1991).
- **Interchange instability:**
 - Driven by gradients in magnetic pressure in plasma in the areas where the confining magnetic field is curved.
 - The name refers to the action of the plasma changing position with the magnetic field lines without significant disturbance to the geometry of the external field.



A simple toy model for MRI. Two small masses connected by a spring orbiting a central mass. In highly conductive plasmas, the magnetic field acts as the spring, giving rise to magnetorotational instability.

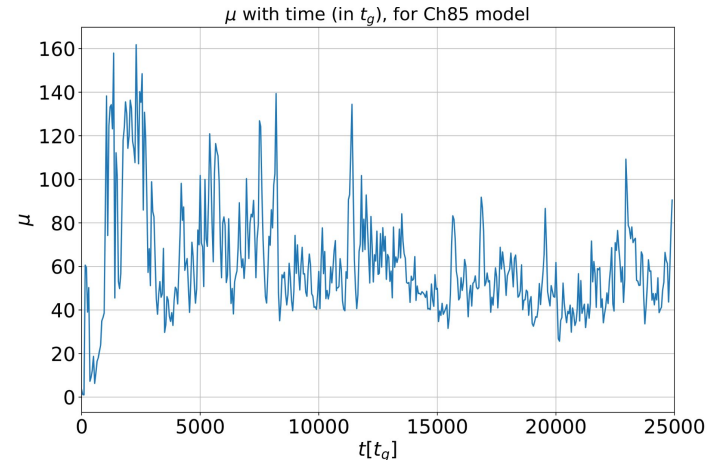
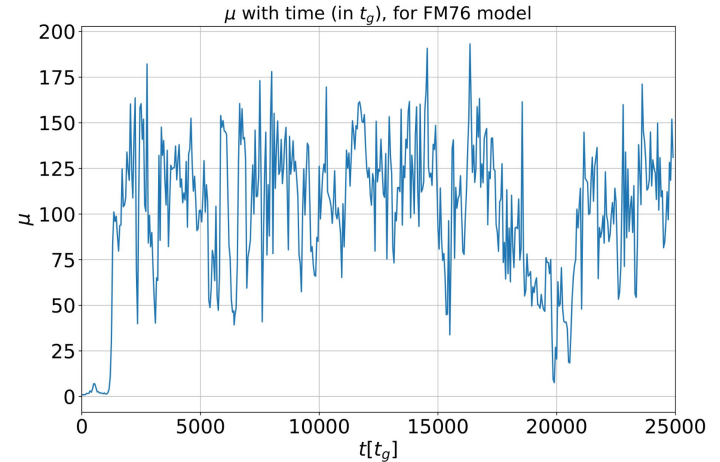
Studying the Jet Variability

- We use the jet energy parameter

$$\mu = -T_t^r / \rho u^r,$$

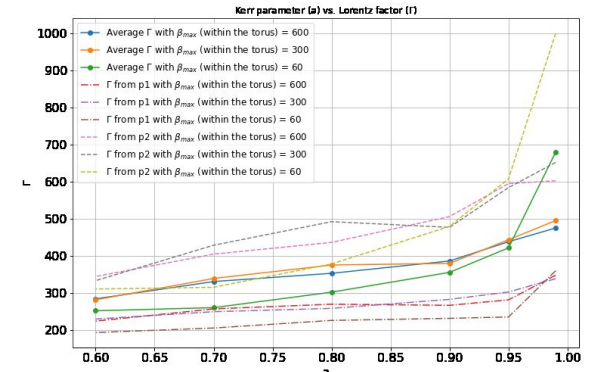
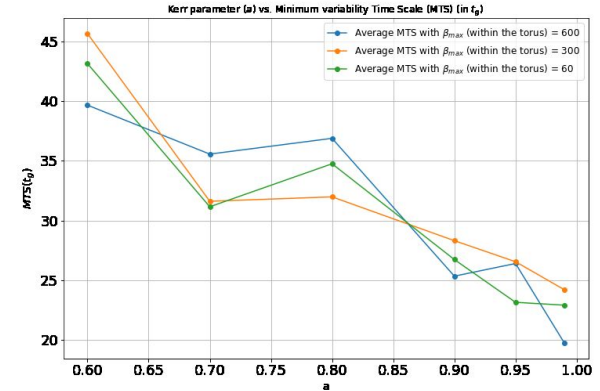
to study the variability of the jet emission
(Sapountzis and Janiuk, 2019)

- It can also provide an estimate of the maximum achievable Lorentz factor $\Gamma_\infty = \mu$, assuming that all the Poynting and the thermal energy is transformed to baryon bulk kinetic (Vlahakis and Königl, 2003; Sapountzis and Janiuk, 2019).
- Minimum variability Time Scale (MTS) \sim peak widths at their half maximum on the μ - t plot



MTS- Γ correlations for GRBs and Blazars

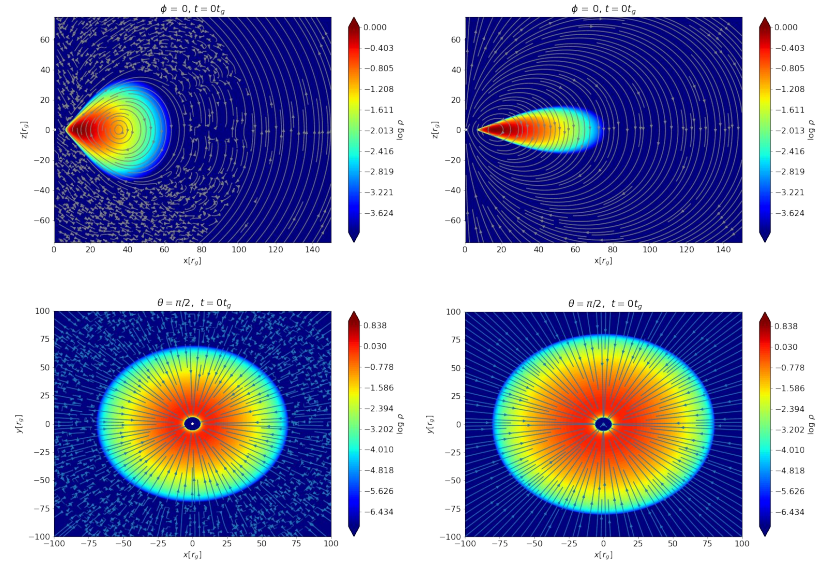
- We computed 2D models, and explored the dependence of jet variability time scale on the values of BH spin and disk initial magnetization (quantified by plasma β).
- Since our models are scale independent, we can scale our results with the black hole mass for the case of GRBs as well as Blazars.
- We investigated the correlations between the Kerr parameter a and minimum variability timescale (MTS) and also with the jet Lorentz factor (Γ).
- We find that the anti-correlation between MTS and the jet Lorentz factor as observed by Wu et al. (2016) can be confirmed by our models.



Ref.: Janiuk, James & Palit (2021)

Numerical Setup

- We explore the scenario of magnetically driven accretion and jet variability related to the formation of the magnetically arrested accretion disk state
- The initial condition of our models assumes the existence of a pressure equilibrium torus, embedded in a poloidal magnetic field.
- Torus initial configurations prescribed according to Fishbone & Moncrief (1976) (model: FM76) and Chakrabarti (1985) (model: Ch85) analytic solutions of equilibrium disks. They differ in the angular momentum distribution inside the disk
- In Ch85, the angular momentum distribution has a power law relation with the parameter $\lambda = (\ell/\Omega)^{1/2}$, where ℓ denotes the specific angular momentum and Ω denotes the angular velocity.



The initial disk structure in our 3D simulations for our two models. The plots show the density distribution at $t = 0$ for the Fishbone-Moncrief (FM) initial condition (left panels) and the Chakrabarti initial condition (right panels) embedded in poloidal magnetic fields. The overplotted lines show the streamlines of the imposed magnetic fields. The top panels show slices along the polar axis and the bottom panels show slices along the equator.

Numerical Setup

- We consider our FM76 model for the structure of a collapsar disk and Ch85 for the remnant of BNS merger.
- In the FM76 model - initial magnetic field is prescribed in such a way that the field lines follow the contours of density in disk.

$$A_\phi(r, \theta) = r^5 (\rho_{avg} / \rho_{max}) - 0.2$$

- In the Ch85 model - the initial field is prescribed as the magnetic field produced by a circular current at r_{max} . The only non-zero component of the vector potential can be written as

$$A_\phi(r, \theta) = A_0 \frac{(2 - k^2)K(k^2) - 2E(k^2)}{k\sqrt{4Rr\sin\theta}}, k = \sqrt{\frac{4Rr\sin\theta}{r^2 + R^2 + 2rR\sin\theta}}$$

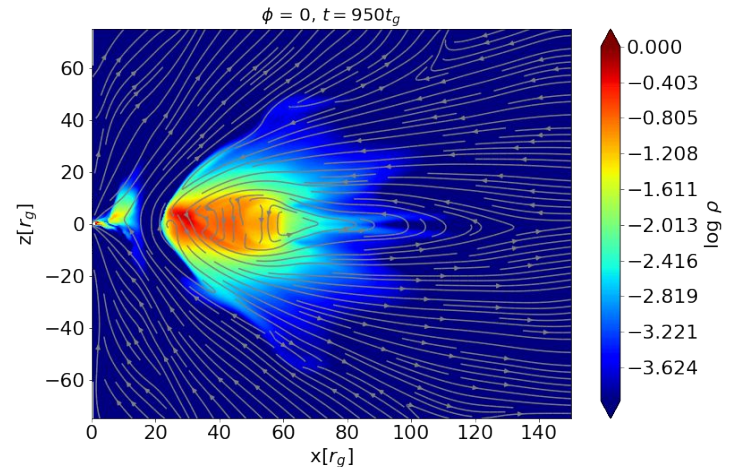
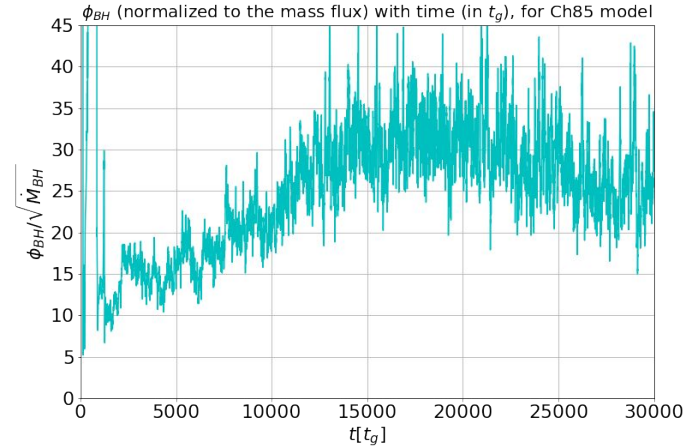
with E and K the complete elliptic integrals, R the position of the circular current in the torus (same as r_{max} in our model) and A_0 a constant parameter.

Magnetically Arrested Disk

- The imposed poloidal magnetic fields results in the development of MRI and starts the accretion.
- The accreting plasma brings along with it more poloidal magnetic field to the black hole (BH) horizon.
- The magnetic flux accumulated on the black hole horizon (normalized to mass flux) can be quantified by:

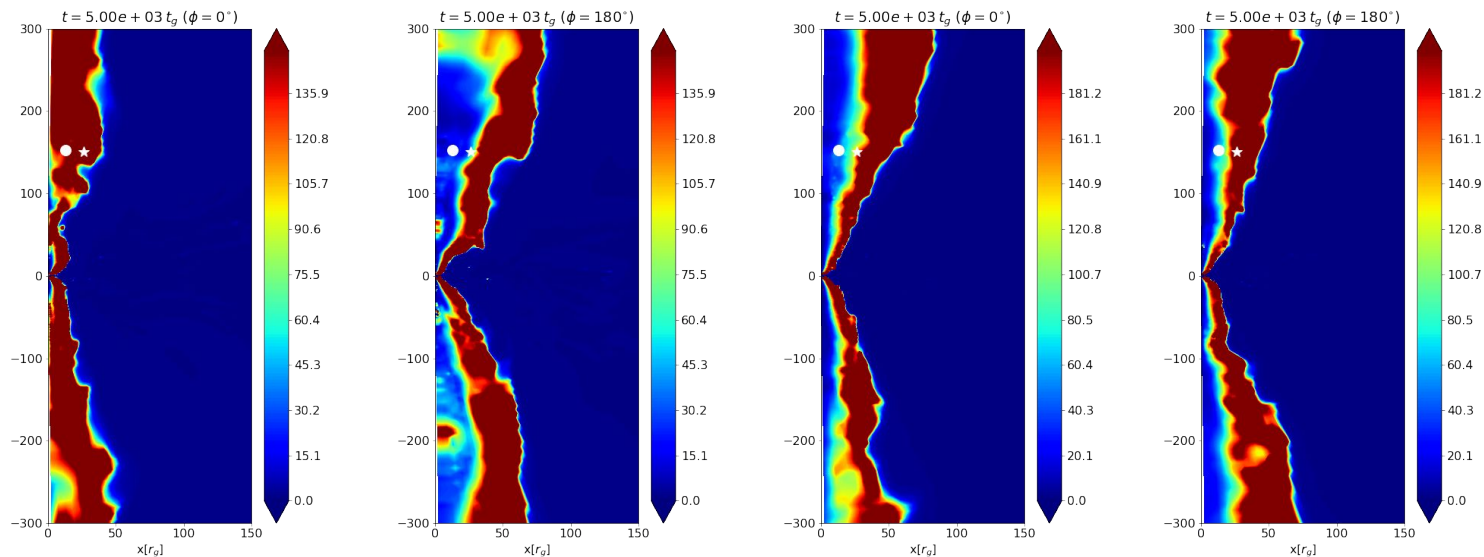
$$\Phi_{\text{BH}} = \frac{1}{\sqrt{\dot{M}}} \int |B^r(r_{\text{hor}})| dA_{\theta\phi}$$

- As time proceeds, this accumulated flux results in a magnetically arrested disk (MAD)
- Further accretion proceeds through other instabilities developed in the plasma



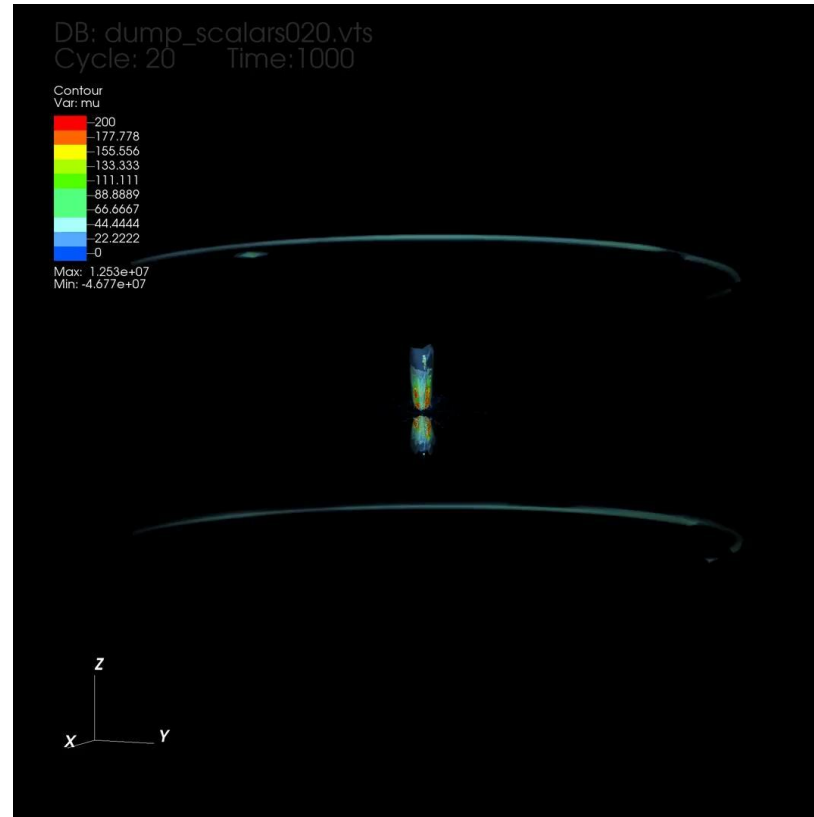
Jet Properties

- We calculate μ at two chosen locations along the jet direction located at $r = 150 r_g$; $\theta = 5^\circ$ (loc. 1) and $\theta = 10^\circ$ (loc. 2) (averaged over ϕ) to measure the time variability



Jet structure at $t = 5000M$ along a 2D slice for FM76 (panels 1 and 2 from left) and Ch85 (panels 3 and 4) models. The marked points show the locations where we measure the variability: circle - location 1 & and star - location 2.

Jet Properties



Jet structure resulting from the FM76 model. The video shows the contours of μ up to a radius of $200 r_g$ and shows the non-axisymmetric structured nature of the jet with a relatively "hollow" core with higher Lorentz factors reached at the edges of the jet far away from the rotation axis of the black hole.

Time Variability

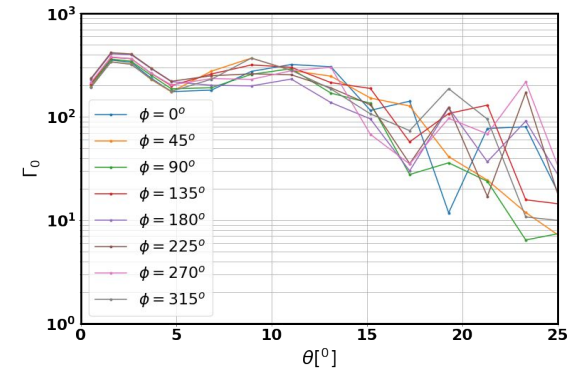
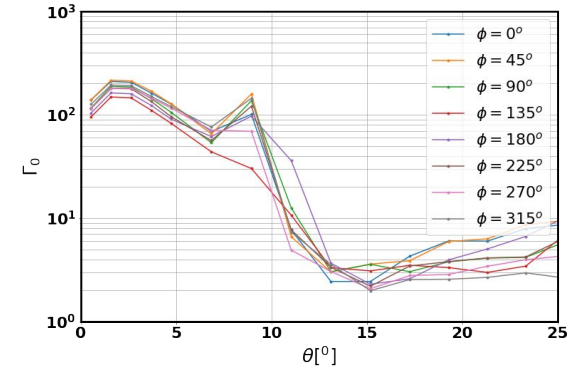
- We investigate the time variability of the jets from the μ variability data computed at the chosen locations.

Model	Lorentz factor (Γ)			MTS estimated (in t_g)			Slope of the PDS	
	Loc. 1	Loc. 2	Average	Loc. 1	Loc. 2	Average	Loc. 1	Loc. 2
FM76	105.96	89.45	97.71	178.63	269.80	224.21	-0.8253	-1.4899
Ch85	61.33	202.36	131.85	147.01	147.72	147.37	-0.8016	-1.1310

- The minimum variability timescale obtained for our short-GRB (Ch85) model is 2.17 ms and for the long-GRB (FM76) model is 13.25 ms. This matches with the observed values from a catalogue of GRB samples (MacLachlan et al. (2013)).
- The slopes of PDS at the chosen points also reveal information about the time variability. From the values, the outer wall of the jet shows higher variability when compared to the inner region of the jet closer to the axis. The slope values are in the lower range as compared to the values for the observed samples (Guidorzi et al. (2016), Dichiara et al. (2016), Dichiara et al. (2013))

Jet Structure

- We compare our models with the observed short and long GRB jet structure and opening angles
- The jets from our models show structured outflows rather than a simple top hat
- The jets produced in our models have a hollow core up to angle $\sim 5^\circ$ at their base and the higher Lorentz factors are reached at the outer edge of the jets, far from the rotation axis.
- We estimate the time averaged jet profile at a large distance of $2000 r_g$ with the polar angle
- The jet in the long GRB (FM76) model has an opening angle $\sim 11^\circ$ and in the short GRB (Ch85) model has an opening angle $\sim 25^\circ$



Time averaged jet Lorentz factor as a function of polar angle, measured at distance of $2000 r_g$ for the model with FM initial condition, for the long GRBs (top) and Chakrabarti initial condition, for the short GRBs (bottom)

Summary

- We investigate the GRB jets in the context of magnetically driven accretion.
- We study the jet structure and temporal variability considering the formation of a magnetically arrested disk (MAD) state as the central engine
- Variability arises in the MAD models from unstable accretion flows mediated by the interchange instabilities and/or magnetic reconnection (Ripperda et al. 2022). This can possibly explain episodic and intermittent jet behaviour.
- Our models produce jets with a hollow core up to an angle of 5° at the base; they have an opening angle of up to $\sim 25^\circ$ for the short-GRBs and up to $\sim 11^\circ$ for the long-GRBs.
- Structured jets consistent with the recent observations. The opening angles we compute are in the range of observed values.
- The disk-jet interaction can result in temporal variability down to a few ms scales. The calculated MTS values are 2.17 ms for the short GRB model and 13.25 ms for the long GRB model.

Ref.: *B. James, A. Janiuk & F.H. Nouri, 2022 (submitted to ApJ), arXiv:2204.01515*

Thank you for your attention.